ELSEVIER

Predictions of axisymmetric and two-dimensional impinging turbulent jets

M. Dianat and M. Fairweather
British Gas plc, Research and Technology, Gas Research Centre, Loughborough, UK

W. P. Jones
Department of Chemical Engineering and Chemical Technology, Imperial College, London, UK

The $k-\varepsilon$ turbulence model and a version of a second-moment closure, modified to include the effect of pressure reflections from a solid surface, have been used as the basis of predictions of the flow that results from the orthogonal impingement of circular and two-dimensional (2-D) jets on a flat surface. Comparison of model predictions has been made with velocity measurements obtained in the stagnation and wall jet regions of the impinging flows. Results, in general, confirm the superiority of the Reynolds stress transport equation model for predicting mean and fluctuating velocities within the latter regions of such flows. In particular, modifications to the second-moment closure to account for the influence of the surface in distorting the fluctuating pressure field away from the wall successfully predict the damping of normal-to-wall velocity fluctuations throughout the impinging flows. In contrast, results derived from the eddy-viscosity-based approach do not, in general, accurately reproduce experimental observations.

Keywords: impinging jets; axisymmetric; two-dimensional; second-moment closure; $k-\varepsilon$ model; velocity field

Introduction

Despite the promise offered by such techniques as direct numerical and large eddy simulations for providing generalised predictive procedures for calculating the turbulent transport of mass, momentum, and heat, their computationally intensive nature currently precludes their use for performing routine engineering calculations. For the foreseeable future, conventional statistical approaches, based on the solution of averaged equations which describe the evolution of mean flow quantities, will continue to be used for the calculation of turbulent transport in the majority of practical flow configurations.

In statistical approaches, the instantaneous flow variables are decomposed into mean and fluctuating quantities, and the resulting equations are averaged in order to convert them into equations for mean flow quantities. As a consequence of the nonlinearity of the equations, however, the averaging process results in a loss of information so that the final equation set is not closed. Closure assumptions for all the second-order moments, including the Reynolds stress and turbulent flux of scalar quantities, must, then, be made before solution is possible. The problem of calculating these moments can be approached at varying levels of complexity, but whilst relatively simple approaches such as those based on the use of a turbulent eddy-viscosity have gained much popularity it appears (Launder 1989; Jones 1990) that second-moment, single-point closures represent the simplest level at which most of the essential features of turbulent flow can be directly described. Such methods, therefore, offer the most likely route forward for providing the widely applicable and generalised predictive procedures required in industrial applications.

In second-moment closures, all the second-order moments are obtained from the solution of modelled partial differential balance, or transport, equations. Many authors have formulated second-moment, single-point closures to the Reynolds stress equation including, for example, Launder et al. (1975), Lumley (1978), and Jones and Musonge (1988). In common with all levels of turbulence model, however, second-moment closures have invariably been developed by reference to turbulent shear flows that are parallel to solid surfaces, and often they are only strictly applicable at distances from a bounding surface that are sufficiently remote for the surface to have a negligible influence on the fluctuating pressure field in the main body of the flow. To improve the generality of turbulence closures there is, therefore, an obvious requirement for models that are applicable irrespective of the flow's distance from, or orientation to, any bounding surfaces.

Recently, Launder and co-workers (Cooper et al. 1993; Craft et al. 1993; Launder and Leschziner 1993) addressed this deficiency through the inclusion in a second-moment closure of additional terms which accounted for the influence of a solid boundary on fluctuating pressures close to the wall and, in particular, modelled the effect of pressure reflections from the surface in dampening velocity fluctuations normal to the wall. The modified closure was then validated against detailed velocity field data obtained from experiments in which turbulent, circular

Address reprint requests to Dr. M. Fairweather, British Gas plc, Research and Technology, Gas Research Centre, Ashby Road, Loughborough LE11 3QU, Leicestershire, UK.

Received 28 August 1995; accepted 18 May 1996

Int. J. Heat and Fluid Flow 17: 530–538, 1996

655 Avenue of the Americas, New York, NY 10010

0142-727X/96/$15.00
PII S0142-727X(96)00076-7

air jets impinged orthogonally onto a large plane surface, with model predictions being in good agreement with observations. The turbulent impinging jet used as the basis of these studies represents a demanding test case for any turbulence model and, more specifically, provides a flow which differs in many important respects from the parallel-to-wall flows more normally used for model development and validation purposes. In particular, and in contrast to flows parallel to surfaces, impinging jets contain regions (close to the axis of symmetry) where turbulence energy is created by normal straining (rather than by shear), and have fluctuating velocities normal to the wall larger than those parallel to it.

The present authors (Dianat et al. 1996) have also extended the second-order, single-point closure model originally proposed by Jones and Musonge (1988) to cover flows that are close to solid surfaces. The influence of such surfaces was modelled through the incorporation of an additional contribution, or wall reflection term, in the modelled form of the redistributive fluctuating pressure term used in the Reynolds stress transport equation. In keeping with the original closure approximation of Jones and Musonge, this reflection term is associated with the mean rate of strain and is linear in the Reynolds stress. Predictions of the extended model were compared with data obtained in a two-dimensional (2-D), flat boundary layer flow (Klebanoff 1954) and an impinging jet (Cooper et al. 1993) with good agreement being found.

Prior to using any model of turbulent transport in performing routine engineering calculations, it is necessary to assess its accuracy and generality through application to a number of flows. The work described in the present paper does this and extends the earlier study noted above by comparing predictions of the modified closure formulation of Jones and Musonge (1988) with a wide range of impinging jet data and with results obtained from the more frequently used k-ε turbulence model. This flow configuration was chosen not only because of its value as a test case for turbulence models, as noted above, but also due to its importance in many industrial applications such as cooling, heating, and drying, as well as in assessments of the consequences of gas releases on both onshore and offshore installations. Predictions of these models are compared with data obtained in a number of different laboratories and, in particular, with measurements on impinging axisymmetric jets obtained by Poreh et al. (1967), Donaldson et al. (1971), Cooper et al. (1993) and Birch et al. (1996) and with data on a 2-D channel flow gathered by Yoshida et al. (1990). Taken together with earlier studies (Jones and Musonge 1988; Dianat et al. 1996) the results presented demonstrate that the extended second-moment closure is capable of predicting reliably a wide range of parallel- and normal-to-wall flows and confirm its superiority over the eddy-viscosity–based approach.

Mathematical model

Governing equations

Predictions were based on solutions of the Reynolds-averaged Navier–Stokes equations closed using either the standard k-ε or a Reynolds stress transport equation turbulence model. For solution, the equations were written in a form appropriate to axisymmetric or 2-D planar flows but, for reasons of brevity, are given below in general Cartesian tensor form.

For an incompressible Newtonian fluid, the conventional time-averaged forms of the partial differential equations which describe the conservation of mass and transport of mean momentum may be written as

$$\frac{\partial U_i}{\partial x_i} = 0 \tag{1}$$

and

$$\frac{\mathrm{d}U_i}{\mathrm{d}t} = -\frac{1}{\rho}\frac{\partial P}{\partial x_i} + \frac{\partial}{\partial x_j}\left[\nu\left(\frac{\partial U_i}{\partial x_j} + \frac{\partial U_j}{\partial x_i}\right) - \overline{u_i u_j}\right] \tag{2}$$

with

$$\frac{\mathrm{d}}{\mathrm{d}t} = \frac{\partial}{\partial t} + U_j\frac{\partial}{\partial x_j} \tag{3}$$

This set of equations is only closed when the Reynolds stress $\overline{u_i u_j}$ is approximated through the use of a turbulence model.

Notation

A_{ij}	redistributive fluctuating pressure term
A^w_{ij}	correction term allowing for wall reflection effects
d	pipe diameter or slot width
f_x	length scale function
h	pipe/slot-to-surface separation
k	turbulence kinetic energy
L	length scale
n_i	unit vector normal to surface
P	mean pressure
r	horizontal (radial) coordinate for axisymmetric flows
Re	Reynolds number ($= Ud/\nu$)
t	time
u	fluctuating velocity normal to surface
u_i	fluctuating velocity in ith coordinate direction
U	mean velocity normal to surface
U_i	mean velocity in ith coordinate direction
v	fluctuating velocity parallel to surface (in r- or y-direction)
V	mean velocity parallel to surface
x	vertical coordinate
x_i	three coordinate directions
y	horizontal coordinate for two-dimensional flows

Greek

δ_{ij}	Kronecker delta
ε	dissipation rate of k
κ	von Karman constant ($= 0.41$)
ν	kinematic viscosity
ν_t	turbulent eddy-viscosity
ρ	density
$\sigma_k, \sigma_\varepsilon$	turbulent Prandtl numbers

Subscripts

b	Bulk value
i	ith direction

Superscripts

$'$	r.m.s. value
—	time averaged

In the standard k-ε turbulence model (Jones and Launder 1972) the Reynolds stress is assumed to be related linearly to the mean rate of strain via a scalar eddy-viscosity:

$$\overline{u_i u_j} = \frac{2}{3}\delta_{ij}k - \nu_t\left(\frac{\partial U_i}{\partial x_j} + \frac{\partial U_j}{\partial x_i}\right) \tag{4}$$

where $k = \overline{u_i u_i}/2$ and $\nu_t = C_\mu(k^2/\varepsilon)$. Values for k and ε are obtained from solution of modelled transport equations:

$$\frac{\mathrm{d}k}{\mathrm{d}t} = \frac{\partial}{\partial x_j}\left(\frac{\nu_t}{\sigma_k}\frac{\partial k}{\partial x_j}\right) - \overline{u_i u_j}\frac{\partial U_i}{\partial x_j} - \varepsilon \tag{5}$$

and

$$\frac{\mathrm{d}\varepsilon}{\mathrm{d}t} = \frac{\partial}{\partial x_j}\left(\frac{\nu_t}{\sigma_\varepsilon}\frac{\partial \varepsilon}{\partial x_j}\right) - C_{\varepsilon 1}\frac{\varepsilon}{k}\overline{u_i u_j}\frac{\partial U_i}{\partial x_j} - C_{\varepsilon 2}\frac{\varepsilon^2}{k} \tag{6}$$

where the model constants were assigned standard values (Jones and Whitelaw 1982) of $C_\mu = 0.09$, $C_{\varepsilon 1} = 1.44$, $C_{\varepsilon 2} = 1.92$, $\sigma_k = 1.0$ and $\sigma_\varepsilon = 1.3$.

In second-moment turbulence closures, the Reynolds stress is obtained directly from solutions of modelled partial differential transport equations. The modelled Reynolds stress transport equation used in the present work may be written as (Jones and Musonge 1988)

$$\frac{\mathrm{d}}{\mathrm{d}t}(\overline{u_i u_j}) + \overline{u_i u_l}\frac{\partial U_j}{\partial x_l} + \overline{u_j u_l}\frac{\partial U_i}{\partial x_l} = C_s\frac{\partial}{\partial x_l}\left(\frac{k}{\varepsilon}\overline{u_l u_m}\frac{\partial}{\partial x_m}(\overline{u_i u_j})\right) + A_{ij} + A_{ij}^w - \frac{2}{3}\delta_{ij}\varepsilon \tag{7}$$

with the redistributive fluctuating pressure term being given by

$$A_{ij} = -C_1\frac{\varepsilon}{k}\left(\overline{u_i u_j} - \frac{2}{3}\delta_{ij}k\right) + C_2\delta_{ij}\overline{u_l u_m}\frac{\partial U_l}{\partial x_m} + C_3\left(\overline{u_l u_j}\frac{\partial U_i}{\partial x_l} + \overline{u_l u_i}\frac{\partial U_j}{\partial x_l}\right) + C_4 k\left(\frac{\partial U_i}{\partial x_j} + \frac{\partial U_j}{\partial x_i}\right) - \left(\frac{3}{2}C_2 + C_3\right)\left(\overline{u_l u_j}\frac{\partial U_l}{\partial x_i} + \overline{u_l u_i}\frac{\partial U_l}{\partial x_j}\right) \tag{8}$$

Here, A_{ij} is modelled as a general linear function of the Reynolds stress tensor, and it is assumed that both the "return" and the mean strain (or "rapid") contribution to the velocity–pressure gradient correlation, normally modelled separately, are directly influenced by mean strain. The model constants were taken as $C_s = 0.18$, $C_1 = 3.00$, $C_2 = -0.44$, $C_3 = 0.46$, and $C_4 = -0.23$ (Jones 1994).

Wall reflection effects were incorporated in the second-order closure of Jones and Musonge (1988) through the A_{ij}^w term in Equation 7. This term represents a correction to the standard redistributive fluctuating pressure term which is included to allow for the influence of pressure reflections from the surface in distorting the fluctuating pressure field away from the wall. Early attempts at modelling this process were made by Shir (1973), who proposed an approximation involving the normal distance from the wall and depending only on turbulence quantities, and by Gibson and Launder (1978), who derived a more general form, which included both turbulence only and mean strain contributions. The latter model is, however, known to give spurious results when the mean flow is directed towards a surface, because in such situations, the mean strain contribution erroneously leads to an augmentation of the velocity fluctuations normal to the wall. This problem was remedied by Craft (1991) who considered a number of terms involving products of the mean velocity gradient and the Reynolds stress tensor and constructed a form which produced the desired effects in both parallel- and normal-to-wall flows. In the present work, A_{ij}^w was taken as (Dianat et al. 1996)

$$A_{ij}^w = -C_{w1}\overline{u_l u_m}\frac{\partial U_k}{\partial x_m}n_l n_k(n_p n_p\delta_{ij} - 3n_i n_j)f_x(L/n_q x_q) - C_{w2}\overline{u_l u_m}\frac{\partial U_m}{\partial x_k}n_l n_k(n_p n_p\delta_{ij} - 3n_i n_j)f_x(L/n_q x_q) \tag{9}$$

This expression is linear in the Reynolds stress, and hence, consistent with the uniqueness arguments invoked by Jones and Musonge (1988) in constructing the linear form of A_{ij}. Its basic form is redistributive and involves terms associated with the mean rate of strain, which, according to recent findings (Brasseur and Lee 1987), are of greater significance than terms involving fluctuating velocities alone. The latter work also demonstrated that the "return" part of the pressure-rate of strain term is associated with much finer scale motions than the "rapid" component, and, hence, that the "rapid" component might be expected to be more affected by the presence of any rigid boundary. In Equation 9, n_i is the unit vector normal to the wall and L is a length scale characterising the energy containing motions. For the impinging flows considered, the function f_x reduces the effect of the wall correction with increasing distance from a surface and was specified, in line with earlier work (Dianat et al. 1991), as $f_x = k^{3/2}/(C_w n_i x_i \varepsilon)$, where $C_w = \kappa/C_\mu^{3/4}$ and C_μ was assigned a value of 0.07 for consistency with equilibrium near wall flows. The constants C_{w1} and C_{w2} were taken as 0.50 and 0.18 (Dianat et al. 1996), these values having been chosen in accordance with data obtained, respectively, in one of the normal-to-wall impinging flows (Cooper et al. 1993) considered further below and in a 2-D, flat boundary-layer flow (Klebanoff 1954). Lastly, the turbulence energy dissipation rate required for solution of Equation 7 was obtained from

$$\frac{\mathrm{d}\varepsilon}{\mathrm{d}t} = C_\varepsilon\frac{\partial}{\partial x_l}\left(\frac{k}{\varepsilon}\overline{u_l u_m}\frac{\partial \varepsilon}{\partial x_m}\right) - C_{\varepsilon 1}\frac{\varepsilon}{k}\overline{u_l u_m}\frac{\partial U_l}{\partial x_m} - C_{\varepsilon 2}\frac{\varepsilon^2}{k} \tag{10}$$

with $C_\varepsilon = 0.15$, $C_{\varepsilon 1} = 1.44$ and $C_{\varepsilon 2} = 1.90$ (Dianat et al. 1996). Here, C_ε has been revised from its normal value in order to maintain consistency with equilibrium wall flows. This also necessitated a change in the value of C_s, used in Equation 7, to 0.18 in order to maintain the ratio C_s/C_ε at its original quoted value.

Computational procedure and boundary conditions

The computational results presented below required solution of the full axisymmetric or 2-D planar forms of the appropriate transport equations. The equations were solved using a modified version of a computer program described elsewhere (Fairweather et al. 1988). The numerical solution method embodied in this program used either cylindrical polar or Cartesian grids and employed a staggered velocity storage arrangement in order to prevent uncoupling between the velocity and pressure fields. A linearised, implicit, conservative difference scheme was used, with convection terms being approximated by the second-order accurate, and bounded, TVD scheme originally proposed by Van Leer (1974). Central differencing was used for all other terms,

and the resulting quasi-linear algebraic equations were solved using a line Gauss–Seidel method, with solution of the velocity and pressure fields being achieved by a pressure correction method.

The experimental arrangement employed in obtaining the data used below for comparison purposes was represented for the computations by a jet issuing vertically downwards from either a circular cross-sectioned pipe or a slot, with the jet impacting orthogonally on a horizontal flat surface. The boundary conditions applied in the computations assumed symmetry along the jet centreline. At the solid surface, no-slip conditions were assumed, with finite-volume solutions being patched onto fully turbulent, local equilibrium wall law profiles with the matching point chosen to be at a fixed distance from the wall for all finite-volume grids used. A full description of the standard method employed, including details of its computer implementation, can be found in Jones (1994). The upper surface of the computational domain was represented either as a wall (for the 2-D flow) or as an entraining constant pressure surface (for the axisymmetric cases), in line with the experimental configurations used, while the remaining boundary was treated for both cases as a constant pressure surface. In performing the calculations, the sensitivity of computed solutions to the positioning of the constant pressure boundaries was investigated, and in the results presented below, these surfaces were located at positions which had a negligible influence on the flow. Initial conditions for the jet were obtained from a separate computation of developing flow in a pipe or slot which used a parabolic marching procedure (Spalding 1977) that was continued downstream until fully developed conditions were reached. This computation was based on the same equation sets described above and used as the basis of the elliptic flow calculations. In deriving initial conditions for the jet studied by Poreh et al. (1967), an effective area was employed for the jet source, as recommended by the latter authors.

Numerical solutions were obtained using expanding finite-volume meshes of up to 102×93 nodes in the horizontal and vertical directions respectively, with the mesh expansion ratio being less than 1.05 in the regions of interest. Results obtained with these grids, and with meshes containing approximately half this number of nodes, demonstrated that the computations were essentially free of numerical error (see, for example, Dianat et al. 1991 and 1996). Results reported in the remainder of the paper were obtained using the more refined meshes.

Results and discussion

Launder and co-workers (Cooper et al. 1993; Craft et al. 1993; Launder and Leschziner 1993) report measurements of the rms of velocity fluctuations normal to a surface along the stagnation line of a number of impinging axisymmetric air jets. Figure 1 compares measurements for a pipe-to-plate separation of $2d$ (for $d = 101.6$ mm), for two jet source Reynolds numbers ($U_b = 3.39$ and 10.33 ms^{-1}), and predictions obtained from the second-moment closure and the $k - \varepsilon$ turbulence model. In this and subsequent figures, a prime (′) is used to denote rms values. In agreement with earlier findings (Craft et al. 1993; Dianat et al. 1996), the standard, two-equation $k - \varepsilon$ model is seen to produce excessive levels of turbulence energy, leading to values of the rms u velocity up to four times as large as those observed in the experiments. This is due to the use of a linear eddy-viscosity–based stress–strain relationship, which leads to the generation of large turbulence energies in the irrotational region close to the stagnation point of the flow. In contrast, predictions of the modified second-moment closure are in excellent agreement with both datasets. In considering these results, it should be noted that the constant C_{w1} used in Equation 9 was assigned a value of 0.50 (Dianat et al. 1996) in order to bring predictions of the model in line with the data given in Figure 1b. Despite this, however, predictions are in accord with observations for both of the flows considered, primarily due to the strong damping effect on the normal-to-wall fluctuating velocities caused by the subtraction of terms (arising from Equation 9) proportional to $\overline{u^2}(\partial U/\partial x)$ from the main redistributive fluctuating pressure term (Equation 8).

Figure 2 compares similar results obtained with axisymmetric jets and increasingly larger pipe-to-plate separations. Figure 2a again gives data obtained by Cooper et al. (1993) for the Re = 70,000 jet, but now for a pipe-to-plate separation of $6d$. Figures 2b and c show, respectively, data obtained by Donaldson et al. (1971) for an impinging air jet with $d = 12.98$ mm, $h/d = 10.0$, and $U_b = 60.96$ ms^{-1}, and data from Birch et al. (1996), who studied an impinging methane jet with $d = 10.80$ mm, $h/d = 12.8$, and $U_b = 119.50$ ms^{-1}. For the latter jet model, results were derived using density-weighted (Favre) averaged forms of the fluid flow equations described earlier. In general, the comparisons of this figure confirm the superiority of results derived from the second-moment closure, with the $k - \varepsilon$ model again producing excessive levels of turbulence energy close to the surface. Differences do exist between the predictions and data given in Figure 2. In particular, some underprediction of rms u velocities by the second-moment closure is apparent in Figure 2a at distances away from the wall. Because the initial conditions for the jet studied by Cooper et al. (1993) are well defined, this is most likely attributable to inaccuracies in the model itself caused by an overprediction of the spreading rate of the free round jet. A similar underprediction of data away from the wall is apparent, at $x/d = 3$, in the results of Figure 2b, although in this case uncertainties in the initial conditions used in the experiments and a lack of measurements in the free jet region of the impinging flow, make it difficult to establish the precise reasons for these inaccuracies. An overprediction of the spreading rate of the free jet may, again, be a contributing factor. Lastly, the results of Figure 2c indicate good agreement between theory and experiment away from the impinged surface, although the second-moment closure apparently underpredicts the datapoint in closest proximity to the wall. The latter datapoint must, however, be treated with some caution (Birch et al. 1996).

Overall, the comparisons given in Figures 1 and 2 demonstrate that, in the irrotational normal straining zone close to the stagnation point, the modified second-moment closure does capture the influence of pressure reflections from the surface in impeding the transfer of energy to the normal-to-wall fluctuating velocity component. This is also the case for increasing levels of near-wall turbulent velocity that occur with increasing pipe-to-plate separations. Away from the stagnation zone and close to

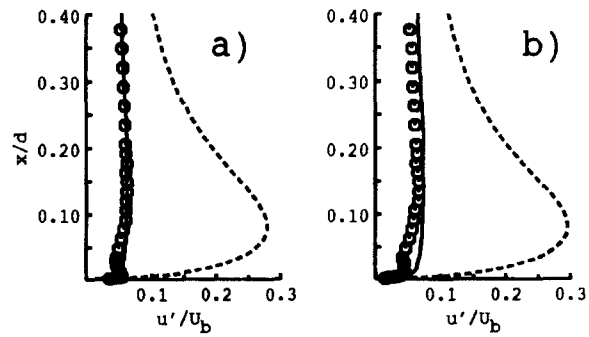

Figure 1 Profiles of rms fluctuating velocity normal to the surface on the stagnation line of the $h/d = 2$ cases studied by Cooper et al. (1993) for a) Re = 23,000 and b) Re = 70,000; (o measured, — predicted second-moment closure, --- predicted k-ε model)

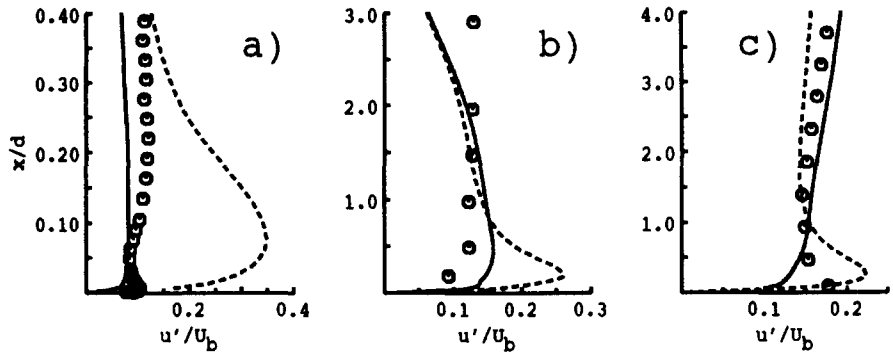

Figure 2 Profiles of rms fluctuating velocity normal to the surface on the stagnation line of the jets studied by a) Cooper et al. (1993), b) Donaldson et al. (1971) and c) Birch et al. (1996); (key as Figure 1)

the edge of the impinging jet, the flow is strongly rotational with large, boundary-induced streamline curvature. Eventually, the flow does revert to a thin shear flow parallel to the surface, or wall jet region, although the flow in this region is by no means simple. In particular, the maximum shear stress occurs outside the near-wall region, with pressure reflections from the surface still impeding the transfer of energy from the streamwise direction to that normal to the surface.

The development of the flow as it moves away from the stagnation point, and shear replaces normal straining as the principal agency for the generation of turbulence energy, is considered in Figures 3–6 for the Re = 23,000, $h/d = 2$ case studied by Cooper et al. (1993). Mean total velocities are given in Figure 3. Along the stagnation line, the mean velocity is dominated by pressure and is not affected significantly by Reynolds stresses. This effect persists up to radial distances approximately equal to the pipe radius, so that predictions derived from both turbulence closures are similar in this region of the flow. Beyond $r/d = 0.5$, however, significant differences start to appear between predictions obtained from the two models, with results derived from the second-moment closure being in excellent qualitative and quantitative agreement with experimental observations, particularly in terms of the location and magnitude of the maximum velocity. In contrast, the $k-\varepsilon$ model tends to underpredict the magnitude of the peak velocity and overestimates the spreading rate in the similarity region of the radial well jet. This effect is attributable to excessive turbulence energy production and mixing close to the stagnation point, which ultimately affects the flow in the radial wall jet, as exemplified by the overprediction of turbulent shear stress within the stagnation region, as shown in Figure 4. In the latter figure, the assumption of an effective turbulent viscosity is seen to lead to reasonable predic-

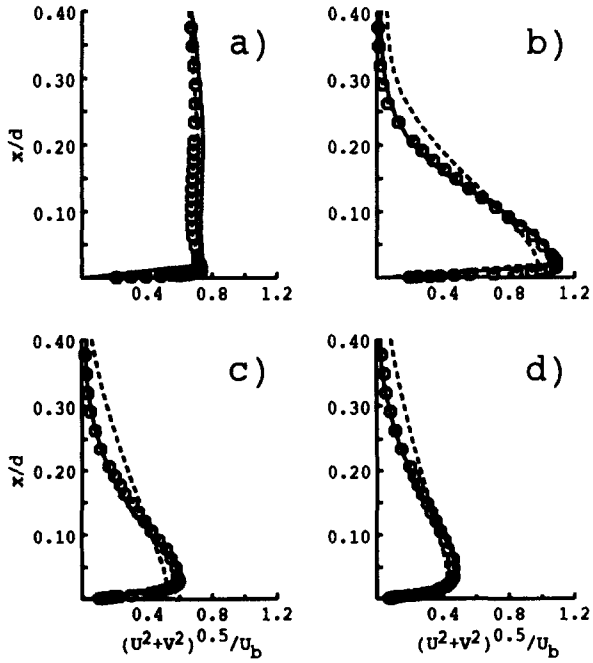

Figure 3 Profiles of mean velocity within the wall jet region of the Re=23,000, $h/d=2$ case studied by Cooper et al. (1993) at a) $r/d=0.5$, b) $r/d=1.0$, c) $r/d=2.5$ and d) $r/d=3.0$; (key as Figure 1)

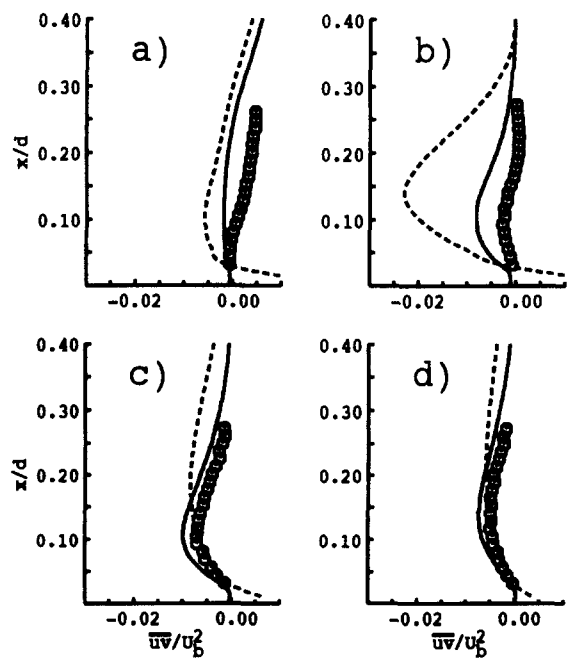

Figure 4 Profiles of shear stress within the wall jet region of the Re=23,000, $h/d=2$ case studied by Cooper et al. (1993) at a) $r/d=0.5$, b) $r/d=1.0$, c) $r/d=2.5$ and d) $r/d=3.0$; (key as Figure 1)

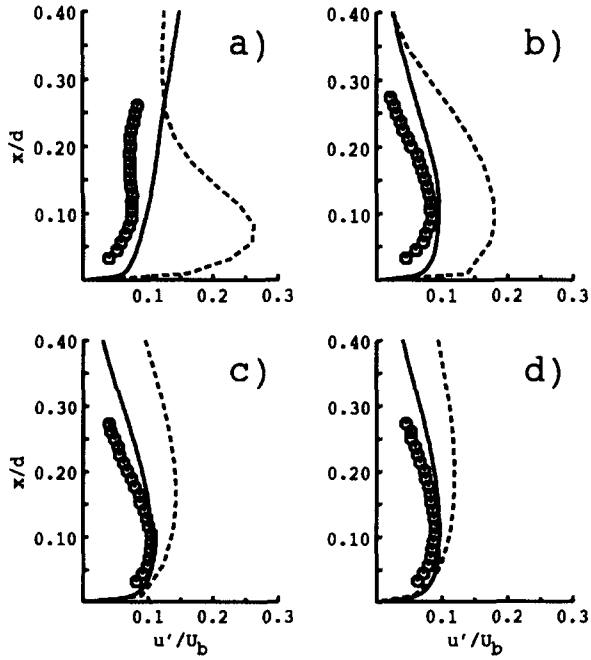

Figure 5 Profiles of rms fluctuating velocity normal to the surface within the wall jet region of the Re=23,000, $h/d=2$ case studied by Cooper et al. (1993) at a) $r/d=0.5$, b) $r/d=1.0$, c) $r/d=2.5$ and d) $r/d=3.0$; (key as Figure 1)

tions of the position of zero shear stress although, overall, results derived from the second-moment closure as in much closer agreement with data throughout the wall jet region.

Fluctuating velocities normal and parallel to the surface are considered, respectively, in Figures 5 and 6. In line with the results of Figure 1a, predictions of the $k-\varepsilon$ model continue to

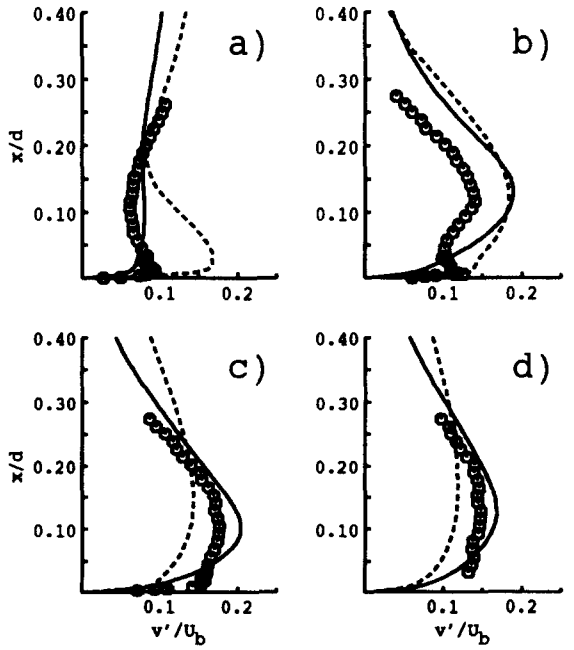

Figure 6 Profiles of rms fluctuating radial velocity within the wall jet region of the Re=23,000, $h/d=2$ case studied by Cooper et al. (1993) at a) $r/d=0.5$, b) $r/d=1.0$, c) $r/d=2.5$ and d) $r/d=3.0$; (key as Figure 1)

overestimate maximum normal-to-wall fluctuating velocities within the stagnation region, although this trend also continues (particularly at large x/d values) with increasing radial distance despite the fact that the inadequacies of the latter model should become less important as shear replaces normal straining as the main agency for turbulence energy generation. This discrepancy can be attributed to the failure of all turbulence models based on the Boussinesq stress–strain relation to account adequately for the sensitivity of the wall jet to streamline curvature effects induced by the lateral divergence of the flow, particularly in view of the underestimation of mean velocity gradients (Figure 3) by the $k-\varepsilon$ model. In contrast, the modified second-moment closure is in good agreement with data on normal-to-wall velocity fluctuations throughout the wall jet region, despite the decreasing influence of pressure reflection effects with increasing radial distance. Lastly, Figure 6 also indicates the superiority of the modified second-moment closure for predicting the radial fluctuating velocity component. Results in the near field of the wall jet do fail to capture the near-wall maxima in this velocity component, although this discrepancy is caused by the use of equilibrium near-wall profiles to describe flow within the low Reynolds number, viscous sublayer region close to the surface, rather than by the second-moment closure itself.

Predictions made for the Re = 70,000 jet at $h/d=2$ and 6 also studied by Cooper et al. (1993), considered further in Dianat et al. (1966), and for the Re = 23,000, $h/d=6$ case showed virtually no influence of Reynolds number or pipe-to-plate separation on the level of agreement achieved with experimental data.

Preh et al. (1967) also studied the impingement of an axisymmetric air jet on a plane surface, with $d=50.8$ mm, $h/d=12$, and $U_b=103.63$ ms^{-1}. The data obtained by these authors allow an assessment of the applicability of the turbulence modelling approaches described earlier at greater radial distances within the wall jet region ($r/d=9$ to 24) than is possible using the data of Cooper et al. (1993), and for a larger pipe-to-plate separation. In the near field of the jet, close to the stagnation point, predictions of the two turbulence models confirmed the conclusions reached earlier. Stagnation line rms u velocities determined from the $k-\varepsilon$ model were, therefore, approximately double those obtained from the modified second-moment closure, while at small distances away from the stagnation point, mean and rms u velocities were qualitatively similar to those of Figure 3 and 5, with predictions of the latter model underestimating peak mean velocities and overestimating the spreading rate and rms u velocities obtained from the second-moment closure. Results in the far field region of the radial wall jet, where experimental data are available, are given in Figures 7–10. Overall, the comparisons shown in the latter figures confirm the superiority of results derived from the modified second-moment closure, with predictions of shear stress (Figure 8), and both normal-to-wall (Figure 9) and parallel-to-wall (Figure 10) fluctuating velocities, being in closest accord with the experimental data. Mean velocities obtained from the latter closure also exhibit good agreement with the data (Figure 7), although for this particular impinging release, the spreading rate of the wall jet appears to be slightly underpredicted. The $k-\varepsilon$ model is again seen to overpredict normal-to-wall fluctuating velocities (Figure 9), although in contrast to earlier findings, the magnitude of the maximum mean velocity (Figure 7) is slightly overpredicted, with the location of the peak being unrealistically close to the surface, while shear stresses (Figure 8) are in reasonable agreement with observations. The improved agreement obtained between predictions of the $k-\varepsilon$ model and the experimental data of Poreh et al. (1967), when compared to comparisons with the data of Cooper et al. (1993), may be attributed to the greater distance of

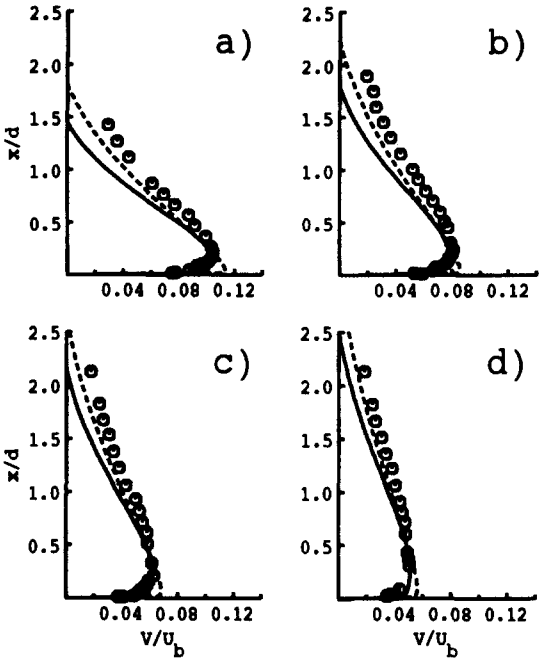

Figure 7 Profiles of mean velocity within the wall jet region of the jet studied by Poreh et al. (1967) and a) $r/d=9$, b) $r/d=12$, c) $r/d=18$ and d) $r/d=24$; (key as Figure 1)

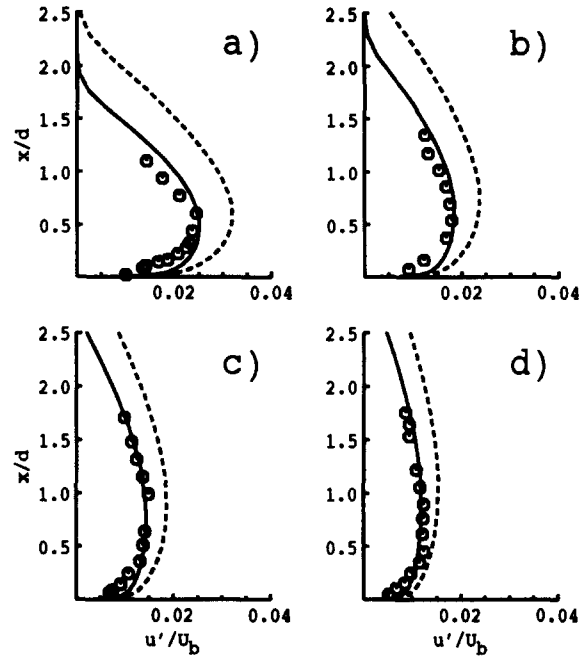

Figure 9 Profiles of rms fluctuating velocity normal to the surface within the wall jet region of the jet studied by Poreh et al. (1967) at a) $r/d=9$, b) $r/d=12$, c) $r/d=18$ and d) $r/d=24$; (key as Figure 1)

the former data from the stagnation region of the impacting jet where the inadequacies of the $k-\varepsilon$ model are reduced.

Lastly, Yoshida et al. (1990) studied the orthogonal impingement of a 2-D channel flow of air on a plane surface. The limited comparisons possible for this case, with $d=10$ mm, $h/d=8$, and $U_b=12.24$ ms^{-1}, are given in Figures 11 and 12. The former figure compares mean velocities close to the stagnation region and in the near field of the wall jet. Unlike earlier results for impinging axisymmetric jets, predictions of the second-moment closure for this planar flow appear to overpredict peak velocities close to the surface, particularly in the near field, despite being in good qualitative agreement with the data. Results derived

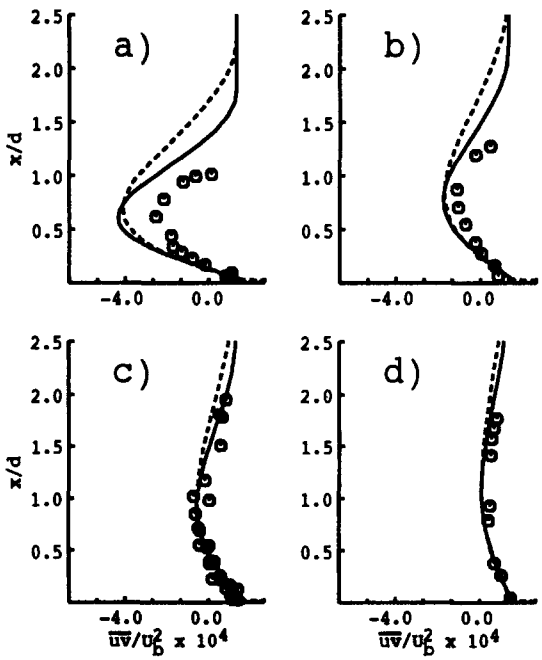

Figure 8 Profiles of shear stress within the wall jet region of the jet studied by Poreh et al. (1967) at a) $r/d=9$, b) $r/d=12$, c) $r/d=18$ and d) $r/d=24$; (key as Figure 1)

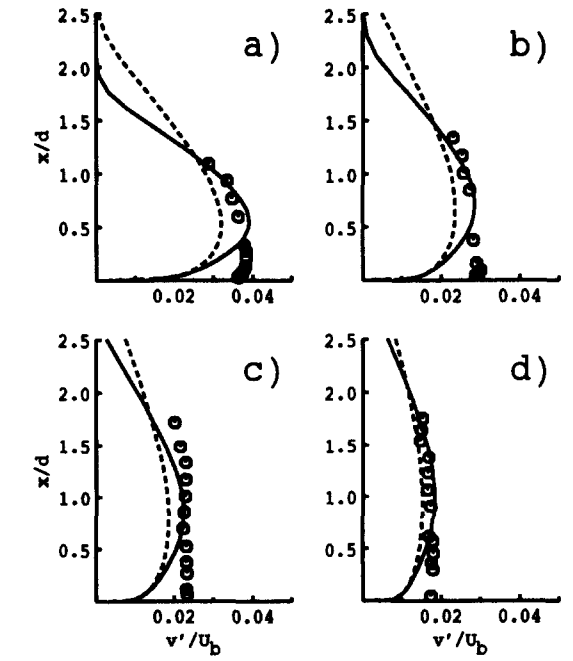

Figure 10 Profiles of rms fluctuating radial velocity within the wall jet region of the jet studied by Poreh et al. (1967) at a) $r/d=9$, b) $r/d=12$, c) $r/d=18$ and d) $r/d=24$; (key as Figure 1)

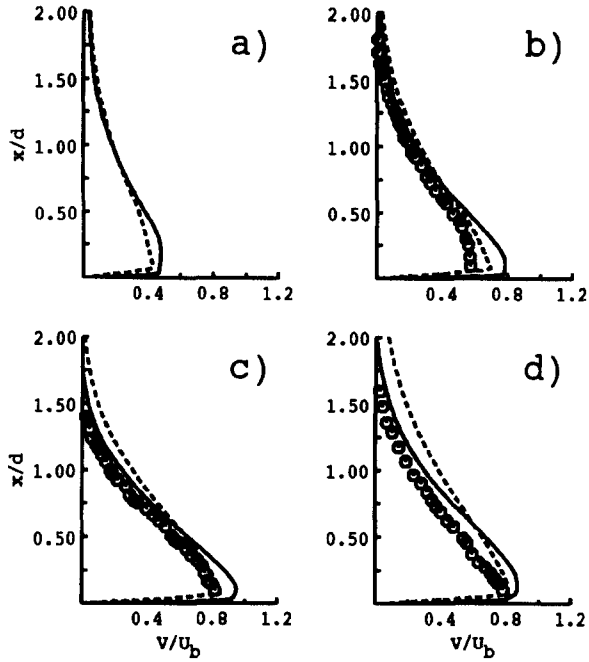

Figure 11 Profiles of mean velocity within the wall jet region of the jet studied by Yoshida et al. (1990) at a) $y/d=0.5$, b) $y/d=1.0$, c) $y/d=2.0$ and d) $y/d=4.0$; (key as Figure 1)

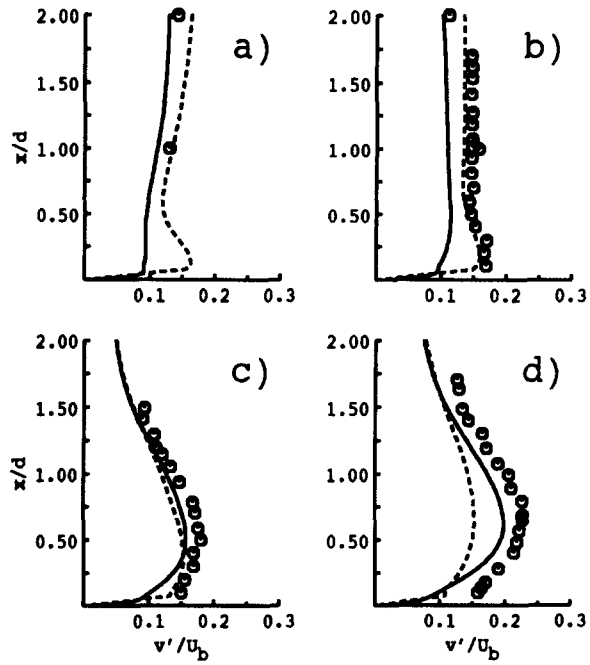

Figure 12 Profiles of rms fluctuating velocity parallel to the surface within the wall jet region of the jet studied by Yoshida et al. (1990) at a) $y/d=0.5$, b) $y/d=1.0$, c) $y/d=2.0$ and d) $y/d=4.0$; (key as Figure 1)

from the k-ε model are in reasonable agreement with maximum velocities although, as for earlier comparisons with the data Cooper et al. (1993), they significantly overestimate the spreading rate of the wall jet. Data for parallel-to-wall fluctuating velocities are compared with predictions of the two models in Figure 12. In contrast with findings for the flow studied by Cooper et al., the eddy-viscosity–based approach appears to perform better close to the stagnation region, although in the near field of the wall jet results derived from the second-moment closure are clearly superior. Close to the stagnation line (Figure 12a and b), however, the data reported by Yoshida et al. (1990) should be treated with some caution, because results derived from different traverses of the flow do exhibit significant scatter (as exemplified by differences between the datapoint at $x/d=2$, and the remaining data, in Figure 12b).

Conclusions

The standard k-ε turbulence model and a version of a second-moment closure, modified to include the influence of solid surfaces, have been used to predict the flow resulting from the orthogonal impingement of axisymmetric jets and a 2-D channel flow on a solid flat surface. Comparison of predictions with measurements made in the stagnation and wall jet regions of these flows demonstrate the superiority of the second-moment closure, with the transport equation model, in general, accurately reproducing observed mean velocities and shear and normal stresses. In particular, modifications to the second-moment closure to account for the influence of the surface in distorting the fluctuating pressure field away from the wall successfully predict the dampening of normal-to-wall velocity fluctuations throughout the impinging flows. In contrast, results derived from the eddy-viscosity–based approach significantly overpredict the latter velocities, particularly in the stagnation region, and, as a consequence (in part), mean and fluctuating velocities throughout the flow are not predicted accurately.

Acknowledgment

This paper is published by permission of British Gas plc.

References

Birch, A. D., Hargrave, G. K. and Shale, G. A. 1996. The turbulent flow field of an impacting jet. (to be published)

Brasseur, J. G. and Lee, M. J. 1987. Local structure of intercomponent energy transfer in homogeneous turbulent shear flow. *Proc. Summer Program, Center for Turbulence Research*, Stanford University, Stanford, CA

Cooper, D., Jackson, D. C., Launder, B. E. and Liao, G. X. 1993. Impinging jet studies for turbulence model assessment—I. Flowfield experiments. *Int. J. Heat Mass Transfer*, **36**, 2675–2684

Craft, T. J. 1991. Ph.D. thesis, University of Manchester, Manchester, UK

Craft, T. J., Graham, L. J. W. and Launder, B. E. 1993. Impinging jet studies for turbulence model assessment—II. An examination of the performance of four turbulence models. *Int. J. Heat Mass Transfer*, **36**, 2685–2697

Dianat, M., Fairweather, M. and Jones, W. P. 1991. Predictions of a turbulent jet impacting a flat surface. *Proc. 8th Symposium on Turbulent Shear Flows*, Munich, Germany

Dianat, M., Fairweather, M. and Jones, W. P. 1996. Reynolds stress closure applied to axisymmetric, impinging turbulent jets. Theoretical and Computational Fluid Dynamics. (in press)

Donaldson, C. DuP., Snedeker, R. S. and Margolis, D. P. 1971. A study of free jet impingement. Part 2. Free jet turbulent structure and impingement heat transfer. *J. Fluid Mech.*, **45**, 477–512

Fairweather, M., Jones, W. P. and Marquis, A. J. 1988. Predictions of the concentration field of a turbulent jet in a cross-flow. *Combust. Sci. and Tech.*, **62**, 61–76

Gibson, M. M. and Launder, B. E. 1978. Ground effects on pressure fluctuations in the atmospheric boundary layer. *J. Fluid Mech.*, **86**, 491–511

Jones, W. P. 1990. Turbulence modelling: Current practice and future trends. *Proc. 1st Int. Symposium on Engineering Turbulence Modelling and Measurements*. Dubrovnik, Yugoslavia

Jones, W. P. 1994. Turbulence modelling and numerical solution methods for variable density and combusting flows. In *Turbulent Reactive Flows*, P. A. Libby and F. A. Williams (eds.), Academic Press, London, 309–374

Jones, W. P. and Launder, B. E. 1972. The prediction of laminarization with a two-equation model of turbulence. *Int. J. Heat Mass Transfer*, **15**, 301–314

Jones, W. P. and Musonge, P. 1988. Closure of the Reynolds stress and scalar flux equations. *Phys. Fluids*, **31**, 3589–3604

Jones, W. P. and Whitelaw, J. H. 1982. Calculation methods for reacting turbulent flows: A Review. *Combust. Flame*, **48**, 1–26

Klebanoff, P. S. 1954. Characteristics of turbulence in a boundary layer with zero pressure gradient. *NACA TN* 3178

Launder, B. E. 1989. Second moment closure: Present and future? *Int. J. Heat Fluid Flow*, **10**, 282–299

Launder, B. E. and Leschziner, M. A. 1993. Description of test cases. *Proc. 2nd ERCOFTAC—IAHR Workshop on Turbulent Flows*, Manchester, UK

Launder, B. E., Reece, G. J. and Rodi, W. 1975. Progress in the development of a Reynolds stress turbulent closure. *J. Fluid Mech.*, **68**, 537–566

Lumley, J. L. 1978. Computational modelling of turbulent flows. In *Advances in Applied Mechanics*, Vol. **18**, C.-S. Yih (ed.), Academic Press, New York, 123–175

Poreh, M., Tsuei, Y. G. and Cermak, J. E. 1967. Investigation of a turbulent radial wall jet. *J. Appl. Mech.*, **34**, 457–463

Shir, C. C. 1973. A preliminary numerical study of atmospheric turbulent flows in the idealized planetary boundary layer, *J. Atmos. Sci.*, **30**, 1327–1339

Spalding, D. B. 1977. *GENMIX: A General Computer Program for Two-Dimensional Parabolic Phenomena*. Pergamon Press, Oxford, UK

Van Leer, B. 1974. Towards the ultimate conservative difference Scheme. II Monotonicity and conservation combined in a second-order scheme. *J. Comp. Phys.*, **14**, 361–370

Yoshida, H., Suenaga, K. and Echigo, R. 1990. Turbulence structure and heat transfer of a two-dimensional impinging jet with gas–solid suspensions. *Int. J. Heat Mass Transfer*, **33**, 859–867